# A fault diagnosis method of turn-to-turn short circuit of permanent magnet synchronous motor (PMSM) based on deep learning

Jiahao Wang, Liuxuan Wei, Manyi Wang[*]

School of Mechanical Engineering, Nanjing University of Science and Technology, Nanjing 210000, China

## ABSTRACT

The fault diagnosis of turn-to-turn short circuit of permanent magnet synchronous motor (PMSM) often results in low diagnostic accuracy due to insufficient sample size. A fault diagnosis method based on deep learning PMSM inter-turn short circuit is proposed. According to the shortcomings of commonly used Generative Adversarial Networks (GAN), fault samples are expanded by using an optimized GAN to build a robust training set. Using stack sparse autoencoder (SSAE) combined with classifier to construct SSAE neural network can effectively solve the shortcomings of SAE's limited learning ability and poor feature learning effect. In this paper, the PMSM three-phase stator current and zero-sequence voltage signals are used as the feature combination for synthetic fault diagnosis. We have conducted extensive experiments on the basis of the above method. The results show that the diagnostic accuracy of this method is as high as 99.4%. Outperforms traditional PMSM turn-to-turn short-circuit fault diagnosis methods.

**Keywords:** PMSM, Optimized GAN, SAE, SSAE, denoising coding

## 1. INTRODUCTION

A frequent problem with permanent magnet synchronous motors is interturn short circuit (PMSM). If the fault is not found in time, it will result in catastrophic failure of the entire drive system and motor operation fault. Deep learning-based PMSM defect diagnostics is therefore extremely important[1, 2]. The primary detection method for inter turn short circuit faults in PMSM is based on zero sequence voltage and stator current. The PMSM control system contains the stator current itself[3]. The zero-sequence voltage is more susceptible to inter turn short circuits than the stator current under the same fault[4]. In order to effectively lessen the impact of external influences on a single characteristic variable, the three-phase stator current and zero sequence voltage signal can be employed as the combined characteristic term of turn-to-turn short circuit fault detection. In addition, fault detection is accomplished using learning techniques such support vector machines (SVM), convolutional neural networks, and sparse self coding networks (SAE)[5-8]. An SAE and a GAN are often generated using[9]. To discover the internal properties of complex data, SAE use unsupervised approaches. However, SAE is a thin network with little capacity for learning. Reference[10] uses SAE depth network and SoftMax classifier to implement six different fault diagnosis methods for asynchronous motors. More than 95% of predictions are correct. The results of document[11] is use of a denoising sparse self coding network to diagnose six asynchronous motor faults are above 97 percent. It is challenging to enable the training of deep learning network model due to the lack of defect examples. To create a significant association between the output data and the input sample data, GAN employs the attack concept. As a result, fault samples can be used to generate fault sample data by being input into GAN. GAN, however, often uses random noise as the generation model's input. The network can only enter a zero-sum game when the data volume is significantly greater than the generation model's parameters, which can quickly result in the demise of GAN mode.

This work proposes a deep learning-based PMSM inter turn short circuit defect diagnosis method based on the aforementioned research. The fault samples are extended using the optimized GAN, then the expanded samples are fed into the SSAE network, where the fault diagnostic and classifier are integrated. This essay suggests the following two approaches to address the aforementioned issues: (1) The trained self encoder (AE) is utilized as the GAN generation model, and the data collected while the motor is operating normally is sent into the GAN model as input. In this approach, network training can be finished, training time can be cut down, and model collapse is difficult even when the amount of fault data is relatively little. (2) To create an SSAE neural network, SSAE is superimposed upon SAE and paired with a classifier. We can naturally combine supervised fine-tuning and unsupervised self-learning to learn the feature expression

[*] manyi.wang@njust.edu.cn

of input data and enhance the network's generalization capacity. The findings of the engineering application demonstrate that this method can precisely categorize and effectively extract the characteristics of the interturn short circuit fault of permanent magnet synchronous motors.

## 2. CHARACTERISTIC ANALYSIS OF PMSM TURN-TO-TURN SHORT CIRCUIT

Collecting stator current signals in three directions with different severity under PMSM turn to turn short circuit fault and signals during normal operation. The waveform is shown in Figure 1a. Orange indicates phase A current; Blue indicates phase B current and green indicates phase C current. By observing Figure 1, it can be concluded that with the increase of the turn ratio of PMSM interturn short circuit fault, the amplitude of phase a current change significantly. The zero-sequence voltage $V$ can be expressed as the voltage difference between the stator winding and the converter, which can be expressed as equation:

$$V = \frac{1}{3} u R_s i_f + \frac{1}{3} u (L + 2M) \frac{di_f}{dt} + \frac{d\lambda_{PM,0}}{dt} \tag{1}$$

In the above formula, $u$ represents the ratio of short circuit turns, $R_s$ represents the three-phase resistance value, $i_f$ represents fault current, $L$ is the self-inductance coefficient, $M$ is mutual-inductance coefficient, $\lambda_{PM,0}$ represents the mean value of back electromotive force of three short circuit windings). Collect the zero-sequence voltage signals of PMSM under normal working state and fault state with different short circuit turn ratio. The waveform is shown in Figure 1b. It is evident that the zero-sequence voltage waveform dramatically alters following the turn-to-turn short circuit malfunction of the PMSM.

## 3. CONSTRUCTION OF DEEP LEARNING MODEL

### 3.1 Optimized generative countermeasure network

The richness of data sets is very important for the training of deep learning. This paper proposes an optimized GAN model. As shown in Figure 2, the trained AE is used as the generation model $G$ of GAN, discriminant model $D$ is usually a multilayer perceptron, the input of $G$ in GAN is the data of normal motor operation, and the input of $D$ is the data generated by $G$ and the real fault data. $D$ and $G$ compete with each other. Finally, $G$ depicts the distribution of fault samples by learning the characteristics of fault samples, and then generates pseudo data similar to it, achieve the purpose of data expansion. Define data parameters such as equation:

$$\left\{ \left( a^{(t)}, c^{(t)} \right), m^{(t)} \right\}_{t=1}^{T} \tag{2}$$

where $a^{(t)}$ and $c^{(t)}$ are the *t*-th fault sample and the *t*-th normal sample respectively, $m^{(t)}$ belongs to [1,0], which means that the profile that judges the sample data as true is 1, and the profile that judges the generated data as true is 0. $T$ represents the total number of samples). Relationship between $G$ and $D$ such as equation:

$$m = \begin{pmatrix} D(a) \\ D(\bar{a}) \end{pmatrix} = \begin{pmatrix} D(a) \\ D(G(C)) \end{pmatrix} = R^2 \tag{3}$$

In which $\bar{a}$ means generate data. By fixing $G$, The loss function corresponding to $D$ can be obtained, such as equation:

$$loss_D = \min_{\theta^D} \left\{ -\left[ \Sigma_{a \sim P(a)} \log(D(a, \theta^D)) + \Sigma_{\bar{a} \sim P(\bar{a})} \log(1 - D(\bar{a}, \theta^D)) \right] \right\} \tag{4}$$

In the above formula, $\theta^D$ represents the parameters to be optimized in the discrimination model. $a \sim p(a)$ represents the motor sample distribution. $\bar{a} \sim p(\bar{a})$ represents the distribution of generated data). The design requirements of $D$ are: the likelihood of evaluating the created data to be fake is higher than the likelihood of judging the real defect sample to be true. The following are the design requirements for $G$: When $D$ is fixed, the distribution features of the generated data shall, to the greatest extent possible, agree with the real fault samples., and the maximization objective function as equation:
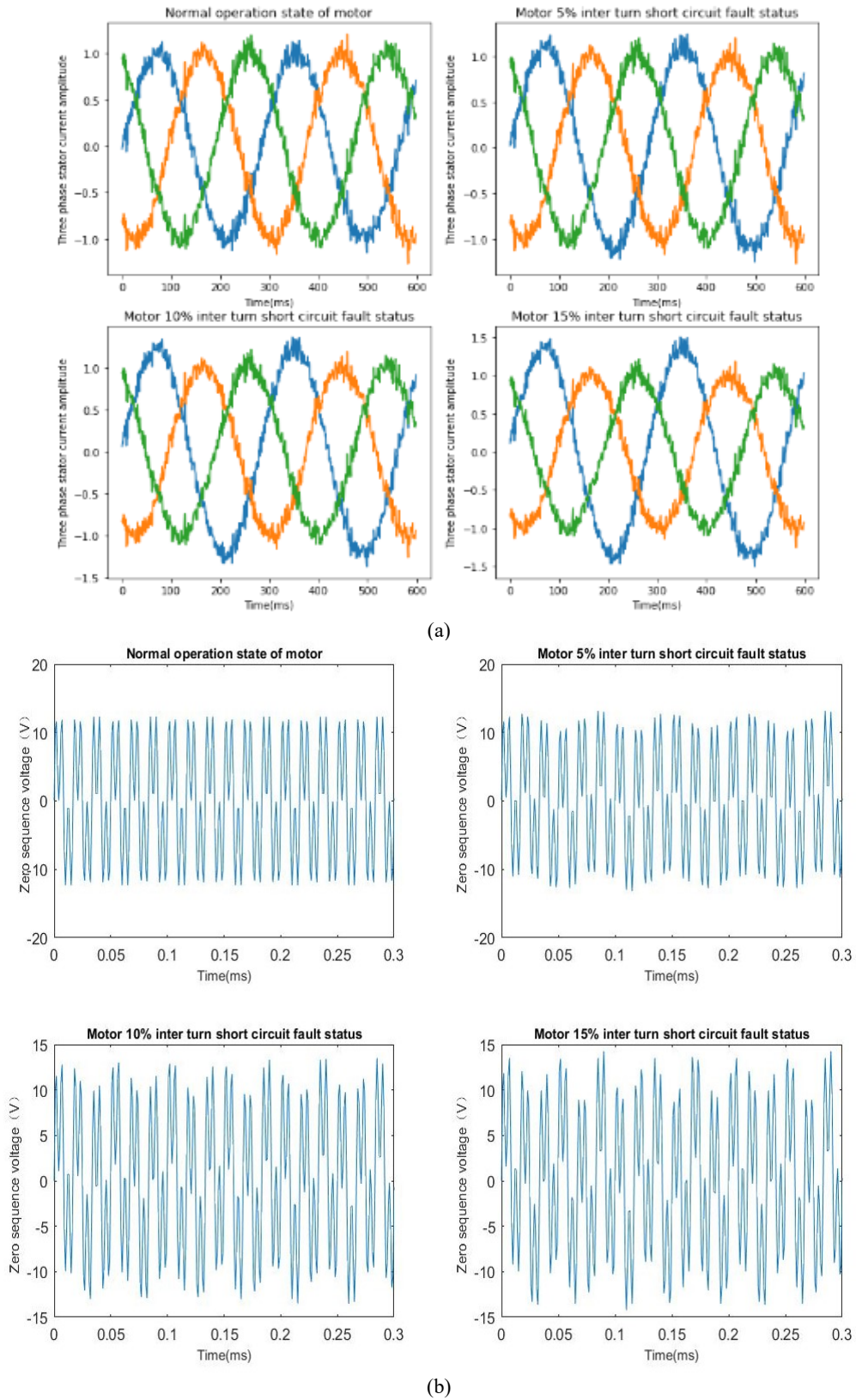
(a)



(b)

Figure 1. PMSM three-phase stator current and zero sequence voltage signal sequence diagram.

$$\max_{\theta^G} = \Sigma_{\bar{a} \sim P(\bar{a})} \log(D(G(c, \theta^G))) \tag{5}$$

$\theta^G$ represents the parameters to be optimized in the generated model. Combining the loss functions of equations (4) and (5), the final objective function of GAN is obtained, as shown in equation:

$$\max_{\theta^G} \min_{\theta^D} J_{GAN}(\theta^G, \theta^D) = \Sigma_{a \sim P(a)} \log(D(a, \theta^D)) + \Sigma_{c \sim P(c)} \log(1 - D(c, \theta^G)) \tag{6}$$

The parameters $\theta^G$ and $\theta^D$ of $G$ and $D$ are optimized by gradient descent to shorten the difference between created and actual data. When $D(G(c)) = 1$, the optimal state is reached between created and actual data.

## 3.2 SSAE neural network

SAE uses regularization strategy to restrict the network on the basis of ordinary AE, so as to improve the generalization ability of the network. The learning ability of the model is limited by adding norm penalty R(θ) to the objective function. At this time, the SAE optimization objective function as equation:

$$\min_{\theta} J_{SAE}(\theta) = \frac{1}{M} \Sigma_{m=1}^{M} \left\| x^{(m)} - x^{(m)} \right\|_2^2 + \delta R(\theta) \tag{7}$$

In the above formula, $\theta$ represents the network parameter set $\{W, b\}$, $W$ represents the parameter weight, $b$ represents the offset vector, $M$ represents the total number of motor samples. $x^{(m)}$ represents the m-th motor sample. $x^{(m)}$ is the prediction of input sample $x^{(m)}$. $R(\theta)$ is a regular term. $\delta$ is a super parameter that weighs the relative contribution between $R(\theta)$ and $J(\theta)$.
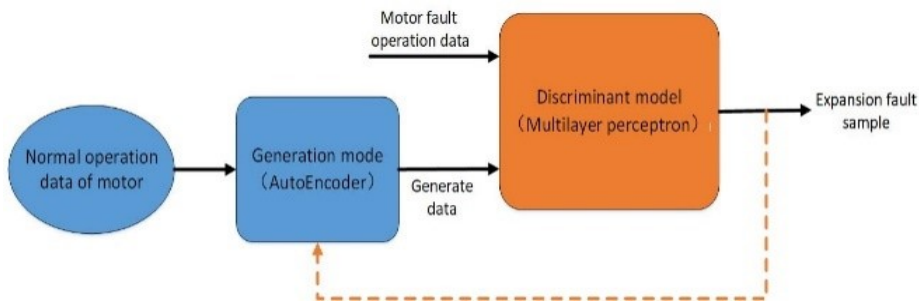


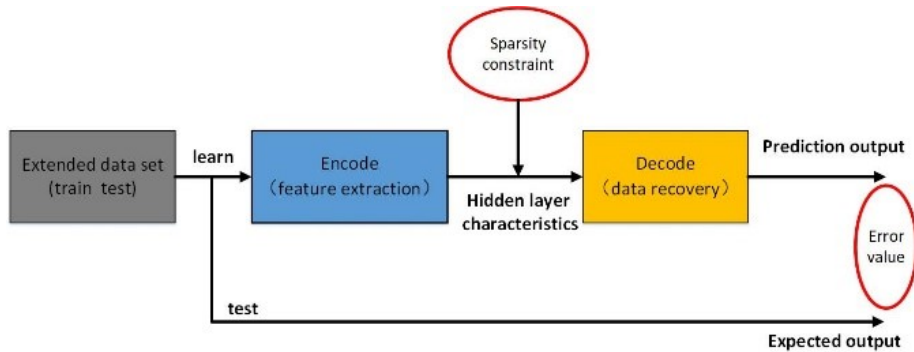Figure 2. Optimized generative countermeasure network.



Figure 3. Sparse self-coding network structure.

The schematic diagram of network structure is shown in Figure 3. In the coding stage, the important features of the input data are extracted, the sparse regular term is introduced, and the $L_1$ constraint is used to punish the output of the hidden layer nodes. In the decoding stage, the extracted features are recovered and the prediction results are output. The reliability

of diagnosis results and actual results is compared by objective function. $L_1$ norm has the advantages of small amount of calculation and convenient operation. Therefore, the optimization objective function of sparse self-coding network based on $L_1$ norm as equation:

$$\min_{\theta} J_{sparse}(\theta) = \frac{1}{M}\sum_{m=1}^{M}\left\|x^{(m)} - x^{(m)}\right\|_2^2 + \delta R(\theta) + \beta\frac{1}{M}\sum_{m=1}^{M}\left\|x^{(m)}\right\|_1 \tag{8}$$

The objective function $J_{sparse}(\theta)$ is minimized through the back-propagation algorithm, and the gradient descent method is used to optimize the parameter weight $W$ and offset $b$ in the process of continuous iteration.

SAE consists of a three-tier network. Only one hidden layer limits the ability of feature extraction. In order to better learn the features with strong representation ability, SAE stack is formed into SSAE, and then a classification layer is added to construct SSAE neural network. The specific scheme is: when multiple SAE are superimposed, the hidden layer of the previous SAE is used as the input layer of the next SAE. Set the network coding phase parameter corresponding to layer $l$ as $\theta_v = \left\{W^{(v,1)}, b^{(v,1)}\right\}$ and the decoding phase parameter as $\theta_v^* = \left\{W^{(v,2)}, b^{(v,2)}\right\}$. For $N$-layer stack networks, the coding sequence is from front to back. The corresponding coding process of each layer as equation:

$$\begin{cases} e^{(v)} = f(y^{(v)}) \\ y^{(v+1)} = W^{(v,1)} \bullet e^{(v)} + b^{(v,1)} \end{cases} \tag{9}$$

($e^{(l)}$ refers to the output of layer $l$, $f(*)$ is the activation function. $y(l)$ and $y(l+1)$ are the input of layer $l$ and layer $l+1$ respectively). if the multi-layer SAE behind the stack performs decoding from back to front, the decoding steps corresponding to each layer as equation:

$$\begin{cases} e^{(N+v)} = g(y^{(N+v)}) \\ y^{(N+v+1)} = W^{(N-v,2)} \bullet e^{(N+v)} + b^{(N-v,2)} \end{cases} \tag{10}$$

($e^{(N+l)}$ is the output of the deepest hidden unit, $g(*)$ is the activation function). The last hidden layer of SSAE can only reconstruct the original data and has no classification ability. Therefore, in order to realize the classification and diagnosis function of inter turn short circuit fault, a classification layer is added after the last hidden layer. The network model is shown in Figure 4. The number of neurons in the classification layer is the number of inter turn short circuit faults with different degrees.
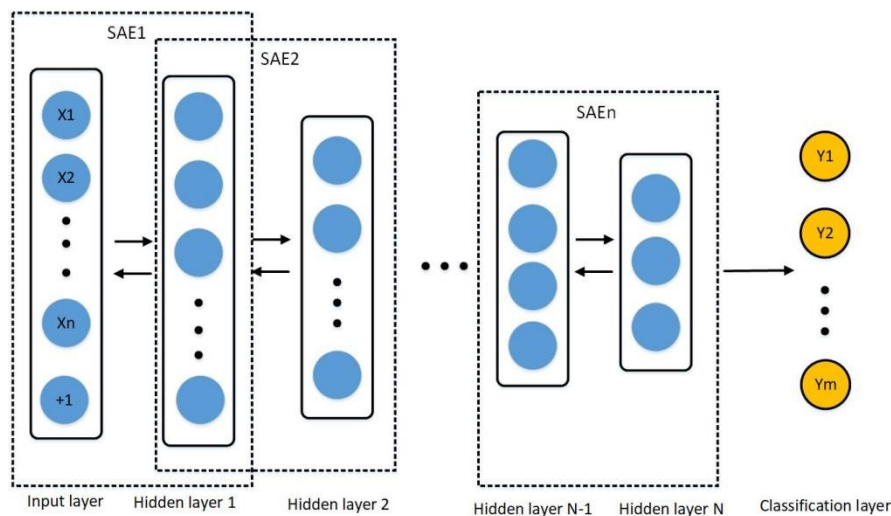


Figure 4. Deep sparse self coding neural network structure.

SSAE neural network includes two training steps: forward network pre training (unsupervised mode) and reverse fine tuning (supervised mode). It is pre trained by layer-by-layer greedy training method. The steps are as follows:

(1) Input the data into the first layer of SAE after preprocessing, and train the first layer of SAE in an unsupervised manner to obtain the parameter weight $W^{(1)}$ and offset $b^{(1)}$.

(2) The hidden layer of the upper layer of SAE is used as the input of the next layer of SAE, and the next layer of SAE is trained to obtain the parameter weight $W^{(2)}$ and offset $b^{(2)}$. of the second layer.

(3) Repeat step (2), take the output of the trained hidden layer of layer ($N$ -1) as the input of layer $N$, obtain the parameter weight $W^{(N)}$ and offset $b^{(N)}$ of the last layer, and complete the training of all SAE.

(4) The output of the last hidden layer is used as the input of the classifier to prepare for the next supervised fine-tuning.

After pre training SAE of each layer through the above steps, establish SSAE network. Monitor and fine tune the network through labeled samples. All layers of SSAE are regarded as a model, and the parameters of SSAE are adjusted by back propagation algorithm. After several iterations, the parameter weight $W$ and deviation $b$ of each layer are optimized. The output of the last hidden layer and the category label are used as the input of the classification layer. The objective function of overall optimization as equation:

$$J(W,b) = \left[ \frac{1}{M} \sum_{m=1}^{M} J(W,b,x^{(m)},h^{(m)}) \right]$$ (11)

$h^{(i)}$ is the fault type label. SSAE organically combines unsupervised self-learning with supervised fine-tuning, which can better extract the deep features of input data. By outputting the probability of fault type in the classification layer, the classification of PMSM inter turn short circuit fault is realized.

## 4. EXPERIMENTAL ANALYSIS

### 4.1 The proposed method

Figure 5 illustrates the deep learning-based fault diagnostic approach used in this study for turn-to-turn short circuits in permanent magnet synchronous motors.
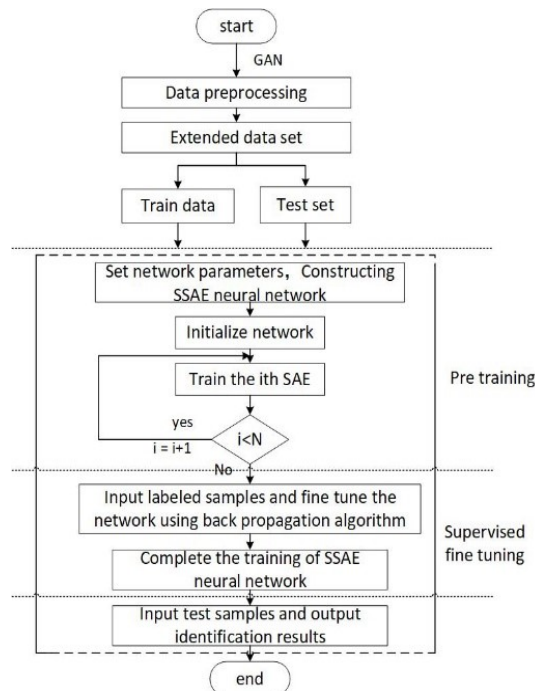


Figure 5. Overall flow diagram of PMSM turn to turn short circuit fault diagnosis.

## 4.2 Experimental description

A permanent magnet synchronous motor experimental test platform is constructed, as illustrated in Figure 6, to confirm the efficacy of this approach. One serves as the load motor, while the other serves as the experimental motor in the utilization of two permanent magnet synchronous motors. We decided to conduct the test when the motor operates at low speed, and the test parameters are stated in Table 1, in order to prevent the motor from suffering long-term damage as a result of high short-circuit current during the test.



Figure 6. PMSM inverter open circuit experiment platform.

Table 1. PMSM parameters.

| Value | Parameters | Parameters | value |
|-------|------------|------------|-------|
| 550W | Rated power (W) | Rated speed (Ω) | 1500 |
| 3.5 | Rated torque (N·m) | Winding turns | 512 |
| 2 | Polar logarithm | Stator resistance | 10.5 |
| 1.5A | Rated current (A) | self inductances (H) | 0.16 |
| 0.636 | Permanent magnet chain (Wb) | Mutua linductances (H) | 0.16 |

We use current sensor to collect PMSM three-phase stator current signal and zero sequence voltage signal. Collect the data of 4000 groups of motors in normal operation and 1000 groups of motors in 5%, 10% and 15% fault operation. After preprocessing the collected data, the real data sets of PMSM with different degrees of inter turn short circuit fault are constructed.

## 4.3 The validity analysis of our method

In order to verify the efficiency of the optimized GAN extended fault sample data proposed in this paper, we use the general GAN and the optimized GAN to extend the real fault samples we collected respectively. The data volume and training batch (training time) required for the training of the two models are shown in Table 2.

As can be seen from Table 2, even when the real data is a small sample, the optimized GAN can complete the training of the network model. However, for general GAN training, the amount of data in the training set should be much larger than the number of parameters in the generator. The training batch of optimized GAN is also less than that of ordinary GAN, indicating that its training time is shorter. The superiority of the optimized GAN proposed in this paper is verified.

We created a 3:1 split between the training and test sets from the real data set, and a fault type label is added to one quarter of the data in the divided training set. Firstly, the training set without label is used for unsupervised pre training of SSAE, and then the training set with label is used for supervised fine-tuning of SSAE. The last hidden layer of SSAE connects the classification layer and outputs the probability value of fault type. The test set verifies the diagnosis efficiency and generalization ability of the network. Considering the influence of the number of SSAE network layers on the diagnosis

results, we construct a multilayer SSAE network, where $N = 1,2,3,4,5$. The recognition accuracy of $N$-layer network is shown in Table 3.

Table 2. A slightly more complex table with a narrow caption.

| Number | General network | | | Optimized network | | |
|---|---|---|---|---|---|---|
| | sample | batch | result | sample | batch | result |
| 1 | 40 | 60 | fault | 20 | 40 | fault |
| 2 | 60 | 80 | fault | 40 | 50 | finish |
| 3 | 80 | 100 | fault | 60 | 60 | finish |
| 4 | 100 | 120 | finish | 80 | 70 | finish |
| 5 | 120 | 140 | finish | 100 | 80 | finish |

Table 3. Curacy corresponding to n-layer network.

| Number of network layers | Accuracy |
|---|---|
| 1 | 90.58% |
| 2 | 94.88% |
| 3 | 94.31% |
| 4 | 84.19% |
| 5 | 76.60% |

The same data is input into SSAE neural network with different network layers, the diagnosis results are obviously different. When the number of network layers is two, the diagnosis accuracy reaches the maximum. From the second layer, with the increase of the number of layers, not only the training time becomes longer, but also the diagnostic accuracy decreases. Therefore, we choose to use two-layer SSAE neural network.

In order to verify the effectiveness of data expansion, the optimized GAN is used to expand three different degrees of inter turn short circuit fault samples, and 1000 groups of pseudo samples are generated respectively. The real data set and pseudo samples are mixed to form an extended data set, with a total of 10000 groups of data. According to the division proportion of the above real data set, the same processing is performed on the extended data set. Based on the same SSAE neural network, the fault diagnosis results under the real data set and the extended data set are compared experimentally, as shown in Figure 7.

As shown in Figure 7, two groups of experiments were carried out. These two groups of experiments used SSAE neural network with the same parameters and the same number of network layers. Experiment 1 used real data sets as network input. Obviously, the insufficient number of samples directly affects the diagnostic efficiency. The accuracy of fault diagnosis tends to decline as sample size increases, and the final diagnosis accuracy is 97.4%. In Experiment 2, the extended data set was used as the network input because the pseudo samples in the extended data set contained irrelevant noise elements. Such samples can improve the generalization ability of the network. It can be seen from the figure that under the same number of samples, the diagnostic accuracy of the extended data set will be slightly higher than that of the actual data set. Too few samples will make the network unable to reach the optimal state. The additional sample set's diagnosis results show that as sample size is increased, the accuracy rate of fault diagnosis begins to stabilize and eventually reaches 99.4%. Therefore, the pseudo data generated by GAN can not only make up for the shortage of network training samples, but also enhance the data set.

We compare this method with conventional ones to show how effective it is. Table 4 displays the comparison's results.
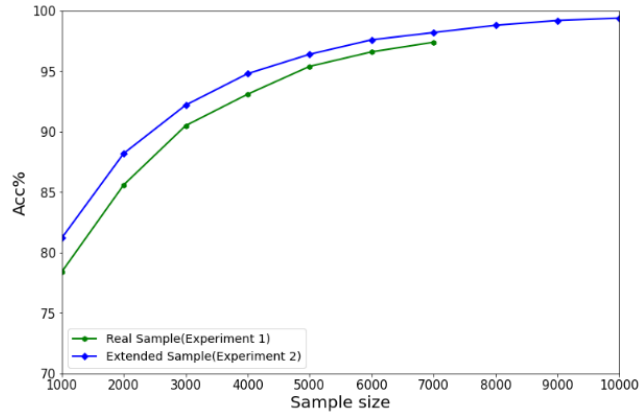
Figure 7. Comparison of diagnostic accuracy under different training sets.

Table 4. Diagnostic results of different training methods.

| Method | Accuracy |
|---|---|
| EMD+SVM | 56.78% |
| SAE | 90.60% |
| 1d-CNN | 91.31% |
| BP neural network | 86.69% |
| Our method | 99.38% |

In the above table 4, the training results of other traditional methods except the method in this paper are from the same real data sets. The combination of EMD and SVM is used for PMSM fault diagnosis. Compared with deep neural network, it has simple structure and convenient calculation, but its efficiency is not as good as other methods. SAE is connected through KL divergence coefficient, and the network generalization ability can be significantly improved and the diagnostic accuracy is satisfactory. But SAE is a shallow network, which still has some room to improve the accuracy of fault diagnosis. One-dimensional convolutional neural network (1D-CNN) is a kind of deep feedforward neural network with local connections and shared weights. It is also a common method in the field of PMSM fault diagnosis. The diagnostic accuracy is also optimistic. BP neural network is a commonly used classification and regression network. The diagnosis results are satisfactory, but the overall efficiency needs to be greatly improved. The combination of optimized GAN and SSAE neural network for fault diagnosis proposed in this paper has the advantage that it not only increases the amount of data, but also enhances the data set by generating noise data in pseudo samples. More robust features are extracted through SSAE neural network, and unsupervised and supervised organic sets are used to improve the generalization ability of the network, prevent the network from over fitting, and finally get more accurate diagnosis results.

## 5. CONCLUSIONS

An effective and precise method for diagnosing PMSM inter turn short circuit faults is presented in this paper. It makes up for the lack of data samples and learning feature ability under the background of deep learning. The innovation of this method lies in:

(1) The optimized GAN is used to extend PMSM in fault samples. Even if the real data set is a small sample, the training of the model can be completed, and the training time can be shortened, which is not easy to lead to the collapse of the model, which greatly improves the shortcomings in the training process of general GAN model.

(2) SSAE neural network deep network adopts the organic combination of unsupervised self-learning and supervised fine-tuning for model training, which can extract more robust feature expression from the input data, so as to improve the diagnosis ability of the network to deal with a variety of data and improve the accuracy of diagnosis.

# ACKNOWLEDGMENTS

# REFERENCES

[1] Ren, H., Qu, J. F., Chai, Y., et al., "Deep learning for fault diagnosis: The state of the art and challenge," Control and Decision, 32(8), 1345(2017).

[2] Xin, P., Ge, B. J., Tao, D. J., et al., "Characteristic law of synchronous generator with stator winding inter-turn short circuit fault," Electric Machines and Control, 23(01), 45(2019).

[3] Gandhi, A., Corrigan, T. and Parsa, L., "Recent advances in modeling and online detection of stator interturn faults in electrical machines," IEEE Transactions on Industrial Electronics, 5(58), 1564-1575(2011).

[4] Fang, J., "Research on initial fault detection method of turn-to-turn short circuit of permanent magnet synchronous motor based on wavelet analysis," Anhui University, (2020). DOI: 10.26917/d.cnki.ganhu.2020.001318

[5] Li, Y. H., Zhao, C. H., Zhou, Y. F., Qin, Y. G., Qin, H. and Su, J. S., "Model predictive torque control strategy of permanent magnet synchronous motor based on convolutional neural network and direct torque control," Motor and Control Applications, (09), 8-15(2020).

[6] Zhang, Z. L., Li, Y. J., Li, M. H. and Wei, H. F., "Fault diagnosis method of permanent magnet synchronous motor based on deep learning," Computer Applications and Software, 36(10), 123-129(2019).

[7] Zhang, Y. X., Xiao, Q. T., Xu, J. X., et al., "Wavelet neural network prediction model based on empirical mode decomposition," Computer Application and Software, 33(10), 284-287(2016).

[8] Mak, M. W. and Rao, W., "Utterance partitioning with acoustic vector resampling for GMM-SVM speaker verification," Speech Communication, 53(1), 119-130(2011).

[9] Li, Y. J., Zhang, Z. L., Li, M. H., Wei, H. F. and Zhang, Y., "Fault diagnosis method of turn-to-turn short circuit of permanent magnet synchronous motor using deep learning," Journal of Electrical Machinery and Control, 24(09), 173-180(2020).

[10] Wang, L. H., Xie, Y. Y., Zhang, Y. H., et al., "A fault diagnosis method for asynchronous motor using deep learning," Journal of Xi'an Jiao tong University, 51(10), 1287(2017).

[11] Sun, W. J., Shao, S. Y. and Yan, R. Q., "Induction motor fault diagnosis based on deep neural network of sparse auto-encoder," Journal of Mechanical Engineering, 52(9), 65(2016).